Behavioral/Cognitive

The Roles of Basolateral Amygdala Parvalbumin Neurons in Fear Learning

Joanna Oi-Yue Yau,[1] Chanchanok Chaichim,[2] John M. Power,[2] and Gavan P. McNally[1]
[1]School of Psychology, University of New South Wales Sydney, Sydney, New South Wales 2052, Australia, and [2]Department of Physiology, Translational Neuroscience Facility, School of Medical Sciences, University of New South Wales Sydney, Sydney, New South Wales 2052, Australia

The basolateral amygdala (BLA) is obligatory for fear learning. This learning is linked to BLA excitatory projection neurons whose activity is regulated by complex networks of inhibitory interneurons, dominated by parvalbumin (PV)-expressing GABAergic neurons. The roles of these GABAergic interneurons in learning to fear and learning not to fear, activity profiles of these interneurons across the course of fear learning, and whether or how these change across the course of learning all remain poorly understood. Here, we used PV cell-type-specific recording and manipulation approaches in male transgenic PV-Cre rats during pavlovian fear conditioning to address these issues. We show that activity of BLA PV neurons during the moments of aversive reinforcement controls fear learning about aversive events, but activity during moments of nonreinforcement does not control fear extinction learning. Furthermore, we show expectation-modulation of BLA PV neurons during fear learning, with greater activity to an unexpected than expected aversive unconditioned stimulus (US). This expectation-modulation was specifically because of BLA PV neuron sensitivity to aversive prediction error. Finally, we show that BLA PV neuron function in fear learning is conserved across these variations in prediction error. We suggest that aversive prediction-error modulation of PV neurons could enable BLA fear-learning circuits to retain selectivity for specific sensory features of aversive USs despite variations in the strength of US inputs, thereby permitting the rapid updating of fear associations when these sensory features change.

Key words: **amygdala; blocking; fear; parvalbumin; prediction error**

Significance Statement

The capacity to learn about sources of danger in the environment is essential for survival. This learning depends on complex microcircuitries of inhibitory interneurons in the basolateral amygdala. Here, we show that parvalbumin-positive GABAergic interneurons in the rat basolateral amygdala are important for fear learning during moments of danger, but not for extinction learning during moments of safety, and that the activity of these neurons is modulated by expectation of danger. This may enable fear-learning circuits to retain selectivity for specific aversive events across variations in expectation, permitting the rapid updating of learning when aversive events change.

Introduction

Animals, including humans, rapidly learn about danger via pavlovian fear conditioning to instruct defensive responses appropriate to the level of threat posed (Fanselow, 1998; Fanselow and Poulos, 2005; Li and McNally, 2014; Yau and McNally, 2018a,b; Wright et al., 2019). The amygdala is essential to this learning. The amygdala mediates learning about how a conditioned stimulus (CS) predicts an aversive unconditioned stimulus (US), and it generates appropriate defensive responses to fear CSs (Maren and Quirk, 2004). Within amygdala, glutamatergic neurons of the basolateral amygdala (BLA) are especially important (Sah et al., 2003). These neurons are strongly recruited by aversive USs, and the activity of these neurons during the moments of reinforcement is obligatory for fear learning (Namburi et al., 2015; Sengupta et al., 2018). The US-evoked activity of these neurons changes across the course of fear learning, reporting the difference between the US expected and the US actually received (i.e., the aversive prediction error; Johansen et al., 2010; McNally et al., 2011; Herry and Johansen, 2014; Ozawa et al., 2017; Ozawa and Johansen, 2018).

The BLA is composed of complex, intrinsic microcircuitries of inhibitory interneurons. These are distinct families of GABAergic neurons defined by expression of a variety of markers (e.g., parvalbumin, somatostatin, cholecystokinin, and vasoactive-intestinal peptide; McDonald, 1992; McDonald and Betette, 2001; Sah et al., 2003). These interneurons dynamically gate BLA projection

Received Sep. 18, 2020; revised Sep. 14, 2021; accepted Sep. 17, 2021.

Author contributions: J.O.-Y.Y., J.M.P., and G.P.M. designed research; J.O.-Y.Y., C.C., and J.M.P. performed research; J.O.-Y.Y., J.M.P., and G.P.M. analyzed data; J.O.-Y.Y. and G.P.M. wrote the paper.

This work was supported by the Australian Research Council (Grant DP170100075) and the University of New South Wales School of Psychology. We thank Pankaj Sah for comments on this manuscript.

Correspondence should be addressed to Gavan P. McNally at g.mcnally@unsw.edu.au.

https://doi.org/10.1523/JNEUROSCI.2461-20.2021

neuron activity, synaptic plasticity, and fear learning (Woodruff and Sah, 2007a,b; Polepalli et al., 2010, 2020; Wolff et al., 2014; Letzkus et al., 2015; Lucas et al., 2016; Krabbe et al., 2018, 2019). Parvalbumin (PV) interneurons are the most common BLA interneuron subtype (McDonald, 1992; McDonald and Betette, 2001; Sah et al., 2003). They form multiple BLA microcircuits, including PV neuron → projection neuron, projection neuron → PV neuron, and PV neuron → interneuron networks (Woodruff and Sah, 2007b; Wolff et al., 2014). Although well implicated in fear learning (Wolff et al., 2014; Lucas et al., 2016), several key questions about BLA PV neuron contributions to pavlovian fear learning remain unanswered. The activity of PV neurons during fear learning remains uncertain. For example, studies in mice using single-unit recordings show that PV neurons are inhibited by a footshock US to disinhibit BLA projection neurons and presumably allow fear association formation (Wolff et al., 2014). Consistent with this, silencing PV neurons during the US augments fear learning, whereas activating them reduces fear learning (Wolff et al., 2014). By contrast, calcium imaging studies in mice show that many PV neurons are excited, not inhibited, by a footshock US (Krabbe et al., 2019). This is consistent with findings that footshock causes rapid inhibitory synaptic input to restrict action potential generation and firing of BLA projection neurons (Windels et al., 2010). Moreover, whether and how the activity of BLA PV neurons changes across the course of conditioning as animals learn about the CS–US relation, as has been shown for both BLA projection neurons (Johansen et al., 2010) and VIP GABAergic interneurons (Krabbe et al., 2019), is not known. Finally, the role PV interneurons in learning about omission of the US during fear extinction is unknown, despite a well-established role in retrieval of established extinction memories (Trouche et al., 2013; Davis et al., 2017).

Here, we used the PV-Cre rat (Wright et al., 2021) to address these questions. We studied the roles of BLA PV neurons in fear and extinction learning. First, we asked whether key findings from the PV-Cre mouse could be extended to a different species using a different measure of fear learning. Then, we asked whether a role for PV neurons extended to learning about US omission during fear extinction learning. Next, we asked how the US-evoked activity of BLA PV neurons changes across fear learning and whether any such changes could be linked to aversive prediction error. Finally, we studied the role that these dynamic activity changes play in fear learning across variations in prediction error.

Materials and Methods

Subjects

Male PV-Cre LE-Tg(Pvalb-iCre)2Ottc heterozygous rats [Optogenetics and Transgenic Technology Core, National Institute on Drug Abuse (NIDA)], were obtained from the NIDA Intramural Research Program Transgenic Rat Project (Wright et al., 2021) via the Rat Resource and Research Center (catalog #00773) and bred at the Animal Resources Center in Perth, Australia. They were housed in groups of two to four in a colony room maintained on a 12 h light/dark cycle (lights on 7:00 A.M.). Rats were maintained on 15 × g of standard lab chow per day with access to water *ad libitum*. Experiments were approved by the University of New South Wales Animal Care and Ethics Committee and performed in accordance with the New South Wales Animal Research Act 1985, under the guidelines of the National Health and Medical Research Council Code for the Care and Use of Animals for Scientific Purposes in Australia (2013).

Apparatus

Behavioral testing was conducted in Med Associates chambers, 24 cm (length) × 30 cm (width) × 21 cm height, enclosed in ventilated, sound-attenuating cabinets, 59.5 cm (length) × 59 cm (width) × × 48 cm (height). The left sidewall was fitted with a magazine dish where grain pellets (Bio-Serv) were delivered when a lever located 4 cm to the right of the magazine was pressed. A 3 W house light mounted on top of the right wall provided illumination in the chamber throughout every session. An LED light mounted on the roof of the sound-attenuating cabinet was used to deliver a flashing visual CS. A speaker attached to the right-side wall of the chamber was used to deliver an auditory CS (CS). A metal grid was fitted to the floor of the chamber to deliver the scrambled footshock US. For optogenetic experiments, an LED driver with an integrated rotary joint (Doric Instruments) was suspended above the center of the operant chamber.

Surgeries and viral vectors

Rats were anaesthetized via 1.3 ml/kg ketamine (Ketamil, Ilium; 100 mg/ml) and 0.3 mg/kg xylazine (Xylazil, Ilium; 20 mg/ml). They received carprofen (Rimadyl, Zoetis) subcutaneously and 0.5% bupivacaine under the incision site. A 5 µl, 30 gauge conical tipped microinfusion syringe (SGE Analytical Science) was used to infuse 0.75 µl of adeno-associated virus (AAV) vectors into BLA (anteroposterior, −3.00; mediolateral ±5.00; dorsoventral, −8.15 mm from bregma; Paxinos and Watson, 2007) at a rate of 0.25 µl/min (UltraMicroPump III with SYS-Micro4 Controller, World Precision Instruments), and the syringe was left in place for an additional 7 min. At each craniotomy, a fiber optic ceramic cannula (Thorlabs) was lowered into the BLA (anteroposterior, −3.00; mediolateral ±5.10; dorsoventral, −8.00; Paxinos and Watson, 2007) and secured in place by dental cement anchored to the screws and the skull. The incision was sutured, and antibiotic (Duplocillin, Intervet) was applied intraperitoneally. Rats were monitored until the end of the experiment.

The Cre-dependent AAV vectors used were the following: AAV5-ef1-DIO-eYFP (3.3×10^{12} GC/ml), pAAV-Ef1a-DIO EYFP was a gift from Karl Deisseroth (Addgene viral prep catalog #27056-AAV5, Addgene; RRID:Addgene_27056); AAV5- ef1α-DIO-hChR2(H134R)-eYFP (5.5×10^{12} GC/ml), pAAV-EF1a-double floxed-hChR2(H134R)-EYFP-WPRE-HGHpA was a gift from Karl Deisseroth (Addgene viral prep, catalog #20298-AAV5, Addgene; RRID:Addgene_20298); AAV5-ef1α-DIO-eNpHR3.0-eYFP (1.1×10^{13} GC/ml), pAAV-Ef1a-DIO eNpHR 3.0-EYFP was a gift from Karl Deisseroth (Addgene viral prep, catalog #26966-AAV5, Addgene; RRID:Addgene_26966); and AAV9-Syn-FLEX-gCaMP7s (1.2×10^{13} GC/ml), pGP-AAV-syn-FLEX-jGCaMP7s-WPRE was a gift from Douglas Kim and the GENIE Project (Addgene viral prep, catalog #104491-AAV9, Addgene; RRID:Addgene_104491).

Procedure

Anatomy. PV-Cre rats with Cre-dependent AAV vectors in the BLA (eNpHR3.0, $n = 5$; eYFP, $n = 3$) were transcardially perfused with saline containing 1% sodium nitrate and heparin (5000 IU/ml) and paraformaldehyde (4%), pH 7.4. Brains were extracted, postfixed (1 h), and cryoprotected in 20% sucrose (48 h). Brains were frozen, and 40 µm BLA sections were sliced and collected on a cryostat (CM 1950, Leica) and stored in a 0.1 M PB saline solution containing 0.1% sodium azide at 4°C. Two-color immunofluorescence was used to reveal PV as well as enhanced yellow fluorescent protein (eYFP) immunoreactivity (IR). Free-floating tissue was washed in PB, pH 7.4, blocked [2 h, 5% NGS in PB containing Triton X-100 (PBTX)], and placed in 1:1500 chicken anti-GFP (catalog #A10262, Thermo Fisher Scientific; RRID:AB_2534023) and 1:1000 mouse anti-PV (catalog #P3088, Sigma-Aldrich; RRID:AB_477329), diluted in a solution of PBTX and 2% NGS at room temperature for 24 h. Sections were washed in PB for 20 min and then incubated in 1:1000 Alexa-488 goat anti-chicken (catalog #A-11 039, Invitrogen; RRID:AB_142924) and 1:750 Alexa Fluor 594 goat anti-mouse (catalog #A-11 032, Invitrogen; RRID:AB_2534091) diluted in PBTX and 2% NGS at room temperature for 2 h. Sections were washed for 30 min in PB, mounted, and coverslipped with Permafluor (Thermo Fisher Scientific). The BLA of each rat was delineated according to Paxinos and Watson (2007) and across two sections, neurons positive for PV-IR and eYFP-IR were assessed via an Olympus BX53 upright microscope (Olympus) and CellSens (Olympus) software and counted using Photoshop (Adobe).

Electrophysiology

Slice preparation. Coronal brain slices (350 μm) were prepared from PV-Cre+ rats that received either AAV5-ef1α-DIO-eNpHR3.0-EYFP or AAV5- ef1α-DIO-hChR2(H134R)-eYFP to BLA. Rats were deeply anaesthetized with isoflurane (5%), decapitated, and the brain removed and placed in ice-cold cutting ACSF containing the following (in mM): 95 NaCl, 2.5 KCl, 30 $NaHCO_3$, 1.2 NaH_2PO_4, 20 HEPES, 25 glucose, 5 ascorbate, 2 thiourea, 3 sodium pyruvate, 0.5 $CaCl_2$, and 10 $MgSO_4$). The brain was trimmed, sliced using a vibratome (model #VT1200, Leica), then incubated for 10–15 min at 30°C in the recovery ACSF containing the following (in mM): 95 NMDG, 2.5 KCl, 30 $NaHCO_3$, 1.2 NaH_2PO_4, 20 HEPES, 25 glucose, 5 ascorbate, 2 thiourea, 3 sodium pyruvate, 0.5 $CaCl_2$, and 10 $MgSO_4$), before being transferred to a Braincubator (Payo Scientific) and held at 18°C in holding ACSF (identical to cutting ACSF but with 2 mM $CaCl_2$ and 2 mM $MgSO_4$). All solutions were pH adjusted to 7.3–7.4 with HCl or NaOH and gassed with carbogen (95% O_2–5% CO_2).

Whole-cell patch-clamp recordings. Slices were transferred to a recording chamber and continuously perfused with standard ACSF (30°C) containing the following (in mM): 124 NaCl, 3 KCl, 26 $NaHCO_3$, 1.2 NaH_2PO_4, 10 glucose, 2.5 $CaCl_2$, and 1.3 $MgCl_2$. Targeted whole-cell patch-clamp recordings were made from eYFP-positive BLA neurons using a microscope (Zeiss Axio Examiner D1) equipped with 20× water immersion objective [1.0 numerical aperture (NA)], LED fluorescence illumination system (pE-2, CoolLED), and an Electron Multiplying Charge-Coupled Device camera (iXon+, Andor Technology). Patch pipettes (3–5 MΩ) were filled with an internal solution containing the following (in mM): 130 potassium gluconate, 10 KCl, 10 HEPES, 4 Mg2-ATP, 0.3 Na3-GTP, 0.3 EGTA, and 10 phosphocreatine disodium salt (pH 7.3, with KOH, 280–290 mOsm). Electrophysiological recordings were amplified using a MultiClamp amplifier (700B, Molecular Devices), filtered at 6–10 kHz and digitized at 20 kHz with a National Instruments multifunction input/output device (PCI-6221). Recordings were controlled and analyzed off-line using Axograph. Liquid junction potentials were uncompensated.

Series resistance and membrane resistance were calculated using built-in routines in Axograph. To determine the passive membrane, action potential (AP) waveform, and neuronal firing pattern, neurons were maintained at −65 mV, and a series of 600 ms current injections (−100–300 pA, 25 pA steps) was applied. The AP threshold was defined as the potential at which the AP velocity exceeded 10 mV/ms. The AP amplitude, half-width, and fast after hyperpolarization (fAHP) were calculated relative to threshold, and eNpHR3.0 was stimulated using orange light (GYR LED bandpass filtered 605/50 nm) delivered through the objective. ChR2 (channelrhodopsin-2) was stimulated using blue light (470 nm LED). To determine the effect of photoinhibition on the AP firing frequency, neurons were induced to fire via depolarizing current injection or trains (5 ms 10 Hz) of depolarizing current injections; the amplitude of current pulse was set to 10 pA above the minimum current required to evoke an AP. When possible, protocols were repeated 5–10 times, and the results averaged. Data were excluded if the series resistance was >20 MΩ or if >150 pA was required to maintain the neuron at −65 mV.

Behavior

Baseline lever-press training. All behavioral experiments used conditioned suppression as a fear measure (Yau and McNally, 2015; Sengupta et al., 2016, 2018). Conditioned suppression has a nonzero baseline because rats lever press for a pellet reward at a constant rate, and they can reveal decreases and increases in fear; there are high levels of baseline activity during training and testing sessions; it is equally sensitive to visual and auditory CSs despite these CSs eliciting different amounts of freezing (Bevins and Ayres, 1991); and assessment is fully automated. All experiments began with lever-pressing training. On day 1, rats received magazine training with lever presses rewarded on a fixed ratio 1 (FR1) schedule in addition to free pellet rewards on a fixed interval 300 s schedule. Magazine training terminated at 60 min, or when the rat reached 100 lever presses. On day 2, rats received FR1 lever-press training. On day 3, lever pressing was maintained on a variable interval (VI) 30 s schedule. From day 4 until the end of the experiment, rats were maintained on a VI 60 s. All sessions lasted 60 min unless otherwise noted. On days 9–10, rats received CS pre-exposure. There were four presentations of each 60 s CS, with an intertrial interval (ITI) between 400 and 720 s. All rats were tethered to dummy patch cables on days 7–9.

Fear acquisition. PV-Cre rats expressing eNpHR3.0 ($n = 8$) or eYFP ($n = 8$) underwent fear conditioning on days 11–14. Before each session, rats were tethered to patch cables outputting at least 10 mW of 625 nm light. Presentation of a 60 s auditory stimulus (85 dB, 1 Hz clicker) coterminated with a 0.5 s, 0.5 mA footshock US. Delivery of 625 nm light (1.5 s) flanked presentation of the US, beginning 0.5 s before shock onset and terminating 0.5 s after shock onset. There were four pairings per session, with an ITI between 500 and 900 s. On day 15 rats were tested for fear response to the CS. The CS was presented four times on a random ITI between 500 and 900 s. For intertrial interval inhibition, eNpHR3.0 ($n = 7$) or eYFP ($n = 8$) groups underwent fear conditioning as described above. Photoinhibition (1.5 s) occurred randomly during each ITI.

To determine the effects of ChR2 excitation on learning, PV-Cre rats expressing ChR2 ($n = 7$) or YFP ($n = 8$). All rats underwent fear conditioning to a 60 s auditory stimulus (85 dB, 1 Hz clicker) paired with a 0.5 s, 0.6 mA footshock US on days 11–13. The timing of photostimulation (1.5 s) flanked the US as described above, but delivery was pulsed at 25 Hz with a 50% duty cycle (20 ms on, 20 ms off). Rats were tested for fear response to the CS on day 14. The CS was presented four times on an ITI between 500 and 900 s.

Fear Extinction. PV-Cre rats expressing eNpHR3.0 ($n = 9$) or eYFP ($n = 7$) underwent fear conditioning to a 60 s tone CS (85 dB, 2800 Hz) on days 11–13, with presentations coterminating with a 0.5 s, 0.6 mA footshock. There were four pairings per day with an ITI of 500–900 s. Rats were tethered to dummy cables on day 11. Fear to the tone was then extinguished across 4 d with four presentations per day and an ITI of 500–900 s. Rats were tethered to patch cables before each extinction session and received continuous delivery of 625 nm light for 5 s at the time of US omission, beginning 0.5 s before tone offset and extending for an extra 4.5 s.

BLA PV responses to signaled versus unsignaled footshocks. PV-Cre rats expressing gCaMP7s ($n = 7$) underwent fear conditioning on days 11–14. During training (days 11–13), rats received four presentations of a 60 s auditory CS (85 dB, 10 Hz clicker) paired with a 0.5 s, 0.6 mA footshock during a 60 min session with an ITI between 600 and 720 s. On test (day 14), rats received four CS–US pairings during an extended 70 min session. In the last 10 min, rats were presented with two unsignaled shocks (760 s and 1200 s after the last CS–US trial). Rats were tethered to patch cables before each session on days 11, 12, and 14 for gCaMP recordings.

Recordings were made using the Fiber Photometry System from Doric Lenses and Tucker Davis Technologies (RZ5P, Synapse), with 465 nm (Ca^{2+}-dependent signal) and 405 nm (isosbestic control signal) emitted from LEDs controlled via dual channel programmable LED drivers (channeled into 0.39 NA, Ø400 μm core multimode prebleached patch cables). Light intensity at the tip of the patch was maintained at 10–30 μW across sessions. gCaMP7 and isosbestic fluorescence were relayed via patch cables, amplified, and measured by Doric Fluorescence Detectors. Synapse software controlled and modulated excitation lights (465 nm, 209 Hz; 405 nm, 331 Hz), as well as demodulated and low-pass filtered (3 Hz) transduced fluorescence signals in real time via the RZ5P. RZ5P/Synapse also received Med-PC signals to record behavioral events in real time.

Fiber photometry during blocking of pavlovian fear. PV-Cre+ rats expressing gCaMP7s were divided into two behavioral groups, Block ($n = 10$) and Control ($n = 9$). All rats were pre-exposed to a CSA (1 Hz flashing LED) and CSB (85 dB, 10 Hz clicker) on Days 9 −10. Each cue was presented four times in a randomized order, with an ITI between 400 and 600 s. Block groups received Stage I training on days 11–13. Presentation of 60 s CSA coterminated with a 0.5 s, 0.6 mA footshock. There were four presentations each day with an ITI between 600 and 720 s. The Control group received VI 60 lever-press training instead. Rats received additional patch cable habituation by being tethered to

dummy cables on the first day of Stage I (day 10). All rats received Stage II training on days 14 and 15. Recordings were made during Stage II. Before each session, rats were tethered to patch cables. In Stage II, CSA was simultaneously presented with CSB, and this 60 s compound cue was coterminated with a 0.5 s, 0.6 mA footshock. There were four presentations each day with an ITI between 600 and 720 s. On day 16, rats were tested for fear response to CSB. CSB was presented four times, with an ITI of 900 s in a 70 min session.

Blocking of pavlovian fear. PV-Cre rats expressing eNpHR3.0 (n = 15) or eYFP (n = 15) were divided into two behavioral groups, Block (eYFP, n = 7; eNpHR3.0, n = 8) and Control (eYFP, n = 8; eNpHR3.0, n = 7). All rats were pre-exposed to CSA (1 Hz flashing LED) and CSB (85 dB, 10 Hz clicker) on Days 9−10. Each cue was presented four times in a randomized order, with an ITI between 400 and 600 s. Block groups received Stage I training on days 10–13 involving presentation of CSA and coterminating with a 0.5 s, 0.6 mA footshock. There were four presentations each day with an ITI between 600 and 720 s. The Control group received VI 60 lever-press training instead. Rats were tethered to dummy patch cables on the first day of Stage I (day 10). All rats received Stage II training on days 14 and 15. Before each session, rats were tethered to patch cables that outputted at least 10 mW of 625 nm light. In Stage II, CSA was simultaneously presented with CSB, and this compound cue coterminated with a 0.5 s, 0.6 mA footshock. There were four presentations each day with an ITI between 600 and 720 s. Photoinhibition was 1.5 s in duration, beginning 0.5 s before shock onset and terminating 0.5 s after shock offset, On day 16, rats were tethered to dummy patch cables before a test session. CSB was presented with an ITI of 900 s in a 70 min session.

Histology

Localization of ChR2, eNpHR3.0, gCaMP7, or eYFP expression was verified using diaminobenzidine (DAB) immunohistochemistry. Free-floating brain tissue was washed in PB, pH 7.4, and rinsed in alcohol (50%), alcohol containing hydrogen peroxide (3%), and normal donkey serum (NDS; 5%) in PB, pH 7.4, for 30 min each. Sections were then incubated in rabbit anti-GFP (1:2000; Life Technologies), diluted in PBTX containing 2% NDS for 24 h at room temperature. After washing off unbound primary antibody, sections were incubated overnight at room temperature in biotinylated donkey anti-rabbit IgG (1:5000; catalog #711–065-152, Jackson ImmunoResearch; RRID:AB_2540016) diluted in 2% NDS PBTX. After washing off unbound secondary antibody, sections were incubated for 2 h at room temperature in ABC reagent (Vector Elite Kit, 6 µ l/ml avidin and 6 µl/ml biotin, Vector Laboratories). Brown GFP-IR cells were revealed using a DAB reaction, with peroxide being generated by glucose oxidase. In this DAB reaction, sections were washed in PB, pH 7.4, followed by 0.1 M acetate buffer, pH 6.0, and then incubated for 15 min in a 0.1 M acetate buffer, pH 6.0, solution containing 0.025% DAB, 0.04% ammonium chloride, and 0.02% D-glucose. The peroxidase reaction was started by adding 0.1 µl/ml glucose oxidase and stopped using acetate buffer, pH 6.0. Brain sections were then washed in PB, pH 7.4, and mounted onto gelatin-treated slides, dehydrated, cleared with histolene, and coverslipped with Entellan (ProSciTech). ChR2, eNpHR3.0, gCaMP7, and eYFP expression sites and cannula placements were determined under a microscope and plotted onto Illustrator (Adobe) templates using boundaries defined by Paxinos and Watson (2007). Rats with unilateral expression/cannula placements or expression/cannula placements outside the boundaries of the BLA were excluded from data analysis.

Experimental design and statistical analyses

Suppression ratios (SRs) were calculated as SR = a/(a + b; Annau and Kamin, 1961), where a is the number of lever presses during the CS, and b is the number of lever presses the minute before the CS (pre-CS period). An SR of 0.5 indicates no suppression (equal number of lever presses during the CS and pre-CS period), whereas an SR of 0 indicates complete suppression, or asymptotic fear. These data and electrophysiology data were analyzed via repeated-measures ANOVA.

Fiber photometry signals were extracted and down sampled (15.89 Hz) before further signal processing. The isosbestic signal was regressed onto the Ca^{2+}-dependent signal to create a fitted isosbestic signal, and a fractional fluorescence (ΔF/F) signal was calculated via subtracting fitted 405 nm signal from 465 nm channels and then further dividing by the fitted 405 nm signal. High-pass (90 s) and low-pass filtering (3 Hz) was conducted. ΔF/F signals around US onset were isolated and aggregated; the 5 s before each event was used as baseline, and the 7 s following each event was defined as the event transient. A bootstrapping confidence interval (CI) procedure (95% CI, 1000 bootstraps) was used to determine significant event-related transients within this window (Jean-Richard-dit-Bressel et al., 2020). A distribution of bootstrapped ΔF/F means was generated by randomly resampling from trial ΔF/F waveforms, with replacement, for the same number of trials. A confidence interval was obtained per time point using the 2.5 and 97.5 percentiles of the bootstrap distribution, which was then expanded by a factor of sqrt(n/(n-1)) to adjust for narrowness bias. Significant transients were defined as periods where 95% CI did not contain zero (baseline) for at least 0.5 s. Areas under the curve (AUCs) for event transients were calculated by approximating the integral (trapezoidal method) of the isolated normalized ΔF/F curves. We analyzed AUCs defined by subject means and by trial means via repeated-measures ANOVA.

Data availability

Data reported here are archived in the University of New South Wales Long Term Data Archive resdata.unsw.edu.au.

Results

AAV expression is specific to BLA PV neurons

We used immunohistochemistry to validate cell-type specificity of AAV expression. PV-Cre rats received BLA infusions of Cre-dependent eNpHR3.0-eYFP (n = 5) or Cre-dependent eYFP (n = 3), and two-color immunofluorescence was used to process BLA sections for eYFP, PV, and eYFP + PV immunoreactivity (IR; Fig. 1*A–C*). There was robust and selective expression of these AAVs in BLA PV neurons, with some encroachment of the AAV into adjacent cortex. There was an average of 116.8 (SEM = 12.4) PV-IR neurons and 54.5 (SEM = 12.2) eYFP-IR neurons per animal with an average of 45% (SEM = 7) of BLA PV-IR neurons transduced. The majority (mean = 98%, SEM = 1) of eYFP-IR neurons also expressed PV-IR (mean dual-labeled neurons per animal = 53, SEM = 11.8; Fig. 1*D*). This confirms the utility of the PV-Cre rat to target BLA PV neurons.

Electrophysiological characterization of BLA PV neurons

Next, whole-cell patch-clamp recordings were made from eNpHR3.0-eYFP- and ChR2-eYFP-expressing BLA neurons from PV-Cre rats (Fig. 2*A,B*). These neurons had membrane resistance (211 ± 15 MΩ), membrane time constant (18 ± 3 ms), brief APs (0.51 ± 0.04 ms), and prominent fAHPs (16.0 ± 1.4 mV), with some firing action potentials in high-frequency bursts with variable interburst intervals (stuttering). These properties are consistent with the known properties of PV neurons (Rainnie et al., 2006; Woodruff and Sah, 2007b). Photoinhibition of eNpHR3.0-eYFP neurons evoked a rapid hyperpolarization persisting for the duration of the light and reliably suppressing PV neuron firing (Fig. 2*C,D*). ChR2-eYFP-expressing neurons were photostimulated (470 nm) with a sustained 1.5 s light pulse or a 25 Hz train of 20 ms light pulses for 1.5 s (Fig. 2*E*). Both protocols reliably evoked AP near the onset of the light pulse, but the 25 Hz train was better to sustain firing throughout the 1.5 s stimulation period (two-way repeated-measures ANOVA; time, $F_{(9,45)} = 5.472$, $p < 0.0001$; light type, $F_{(1,5)} = 2.831$, $p = 0.1533$; interaction, $F_{(9,45)} = 2.261$, $p = 0.0348$; follow-up Sidak comparison, $p = 0.002$; Fig. 2*E,G*)

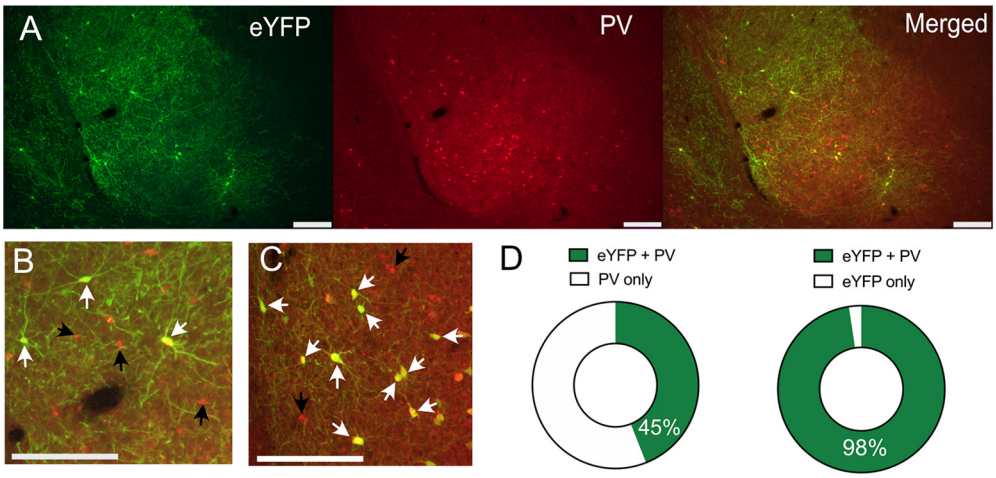

Figure 1. PV neuron-specific transgene expression. PV-Cre rats received BLA infusions of Cre-dependent eNpHR3.0-eYFP ($n = 5$) or Cre-dependent eYFP ($n = 3$). ***A***, Expression of eNpHR3.0-eYFP in BLA PV neurons. ***B***, Higher magnification image showing dual-labeled eNpHR3.0-eYFP/PV neurons. Dual-labeled neurons shown with white arrows, single PV-labeled neurons with black arrows ***C***, Higher magnification image showing dual-labeled eYFP/PV neurons (white arrows) and single PV-labeled neurons with black arrows. Scale bars: 200 μm. ***D***, Nearly half of BLA PV neurons expressed eYFP, and the majority of eYFP neurons were colabeled with PV.

We then recorded from putative BLA projection neurons to assess the effect of PV neuron stimulation on BLA projection neuron firing (Fig. 2*F*,*G*). These eYFP-negative neurons had a lower membrane resistance (116 ± 28 MΩ vs 211 ± 15 MΩ; $t = 3.0$, $p = 0.009$), broader APs (half-width 1.11 ± 0.06 ms vs 0.51 ± 0.04 ms; $t = 7.792$, $p < 0.0001$), and smaller fAHPs (half-width 6.7 ± 1.8 mV vs 16.0 ± 1.4 mV; $t = 3.355$, $p = 0.0043$), than the eYFP-positive PV neurons, and the properties of these eYFP-negative neurons were consistent with BLA projection neurons (Sah et al., 2003). ChR2 stimulation of PV neurons with 470 nm light was sufficient to elicit IPSCs in projection neurons (data not shown) and to inhibit firing (Fig. 2*F*,*G*). We did not observe a difference in the effectiveness of continuous versus pulsed ChR2 stimulation in this inhibition of BLA projection neuronal firing (two-way repeated-measures ANOVA; time, $F_{(15,45)} = 4.464$, $p < 0.000$; light type, $F_{(2,6)} = 3.488$, $p = 0.0989$; interaction, $F_{(30,90)} = 2.939$, $p = 0.0001$).

BLA PV neuron activity at US delivery constrains fear learning

BLA PV interneurons exert strong perisomatic inhibition over BLA principal neurons. In mice this inhibition constrains fear learning. Specifically, optogenetic inhibition of PV neurons during the shock US augments pavlovian fear learning, whereas optogenetic excitation during the shock US impairs pavlovian fear learning as measured by freezing (Wolff et al., 2014). We first asked whether this role of PV neurons can translate across different species as well as across different fear responses by using these same manipulations on pavlovian fear learning in rats using conditioned suppression as the measure of fear. However, in contrast to past work, which relied only on direct comparisons between ChR2 and eNpHR3.0 groups (Wolff et al., 2014), we included non-opsin-expressing controls for each opsin. First, PV-Cre rats received AAVs encoding Cre-dependent eNpHR3.0 ($n = 8$) or eYFP ($n = 8$) and fiber optic cannulae bilaterally into the BLA (Fig. 3*A*,*B*). To establish a steady baseline of lever pressing for conditioned suppression, rats were initially trained to lever press for grain pellets for 10 d and were then preexposed to an auditory CS for 2 d. They then received auditory fear conditioning via pairings of the auditory CS with a 0.5 mA footshock US. We photoinhibited BLA PV neurons only during US delivery via 625 nm light.

Rats acquired fear to the CS across training (linear trend across day, $F_{(1,14)} = 101.891$, $p < 0.001$) with no difference between groups (no main effect of group, $F_{(1,14)} = 1.463$, $p = 0.246$; no group × day interaction, $F_{(1,14)} = 0.003$, $p = 0.960$).

When tested for long-term fear memory 24 h later, the eNpHR3.0 group showed more fear to the CS compared with YFP Control (main effect of group, $F_{(1,14)} = 9.206$, $p = 0.009$), suggesting photoinhibition augmented fear learning (Fig. 3*E*). This augmentation of fear learning was specific to photoinhibition at the time of the shock US because we conducted a separate control experiment where 625 nm light delivery was offset so that rats (eYFP, $n = 8$; eNpHR3.0, n = 7) received delivery of 625 nm light during the intertrial interval rather than during the shock US (Fig. 3*C*). There was no effect of this intertrial interval photoinhibition on fear learning ($F_{(1,13)} = 1.27$ $p = 0.280$) or long-term fear memory on test ($F_{(1,13)} = 0.79$, $p = 0.390$; Fig. 3*F*).

Next, we tested the effect of BLA PV photoexcitation at the time of the shock US. Rats with ChR2 ($n = 7$) or YFP ($n = 8$) expressed in BLA PV neurons underwent 3 d of fear conditioning with an auditory CS paired with a 0.6 mA footshock (Fig. 3*D*, *G*). We used a higher US intensity to increase fear learning in controls and hence optimize detection of any impaired fear learning in ChR2 rats. Rats acquired fear to the CS (linear trend across day, $F_{(1,13)} = 113.769$, $p < 0.001$). Photostimulation at the time of shock US impaired overall fear response to the CS across training (main effect of group, $F_{(1,13)} = 6.654$, $p = 0.023$; Fig. 3*G*). Furthermore, this fear impairment was preserved when fear to the CS was tested 24 h later (main effect of group, $F_{(1,13)} = 9.206$, $p = 0.009$). Together, these findings show bidirectional effects of BLA PV neuron manipulations on fear learning in rats. BLA PV photoinhibition augments fear learning, whereas photoexcitation impairs fear learning.

BLA PV neuron activity at US omission is not necessary for fear extinction learning

Having shown a role for BLA PV neurons at the time of shock US delivery in learning to fear, we next asked whether PV neurons are important at the time of shock omission for learning not to fear. Fear extinction learning remodels PV perisomatic

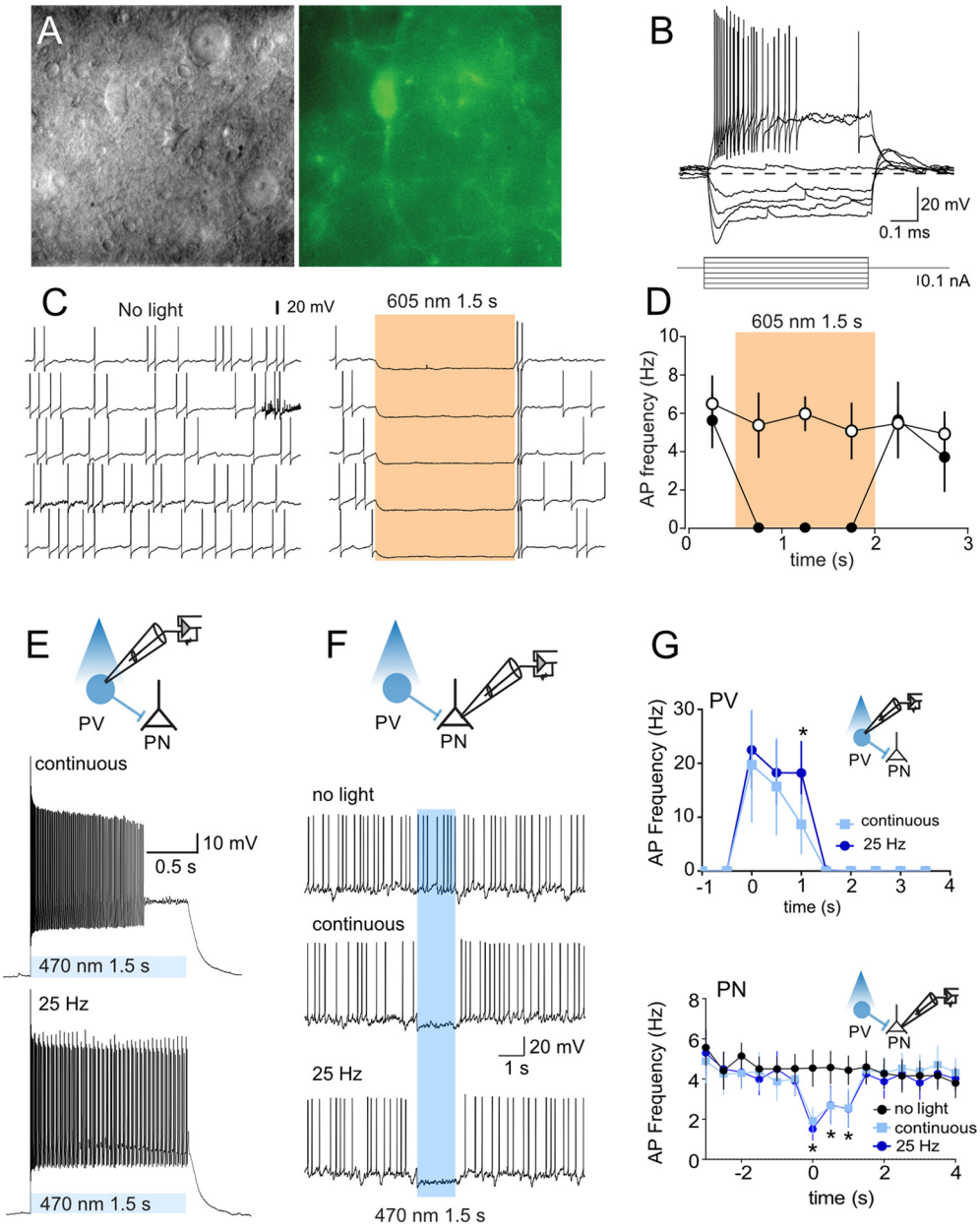

Figure 2. Light-evoked responses of eNpHR3.0 and ChR2 PV BLA neurons. ***A***, Gradient contrast image (left) and green fluorescent image of PV neuron (right). ***B***, Voltage response to current injections. ***C***, Example of light-evoked suppression of PV neuronal firing. ***D***, Mean ± SEM; $n = 6$. PV neuron firing frequency in presence and absence of light stimulation. Shaded areas indicate timing of light presentation. ***E***, Example of light-evoked excitation of PV neuronal firing. ***F***, Example of inhibition of BLA projection neuron (PN) firing by light-evoked excitation of PV neuron. ***G***, Mean PV ($n = 6$) and PN ± SEM; $n = 4$) firing frequency in presence and absence of light stimulation. Twenty-five Hz PV stimulation was better able to sustain PV neuron firing, but there was no difference between these stimulation types in PN neuron inhibition. $^*p < 0.05$.

inhibitory synapses around BLA fear neurons (Trouche et al., 2013; Davis et al., 2017), and recruitment of these BLA PV neurons suppresses fear responding and activity in BLA fear neuronal ensembles during extinction retrieval (Davis et al., 2017; Ozawa et al., 2020). The activity of BLA PV neurons at the time of shock US omission is therefore an obvious candidate for instructing extinction learning, but whether PV neurons serve this role during US omission is unknown.

To study the role of BLA PV neurons in learning about shock omission during fear extinction, PV-Cre rats received application of AAVs encoding Cre-dependent eNpHR3.0 ($n = 9$) or eYFP ($n = 7$) to the BLA. They underwent auditory fear conditioning, then extinction training (Fig. 3*H*). BLA PV neurons were photoinhibited at the time of omission of the expected footshock US during extinction training. Across fear conditioning (data not shown), rats acquired fear to the auditory CS (linear trend across day, $F_{(1,14)} = 75.51$, $p < 0.001$) with no differences between groups (no effect of group, $F_{(1,14)} = 1.45$, $p = 0.248$; or group × day interaction, $F_{(1,14)} = 2.80$, $p = 0.116$), and they also extinguished this fear across extinction training (main effect of day, $F_{(1,14)} = 31.97$, $p < 0.001$). Photoinhibition of BLA PV neurons at the time of shock omission had no effect on fear extinction learning (no main effect of group, $F_{(1,14)} = 0.025$, $p = 0.877$; no group × day interaction, $F_{(1,14)} = 3.502$, $p = 0.082$).

Photoinhibition occurred at the offset of each CS, so the first CS presentation each day serves as a probe to assess extinction retention. We analyzed responding to the first CS of each extinction session (Fig. 3*H*, inset) and found no differences between

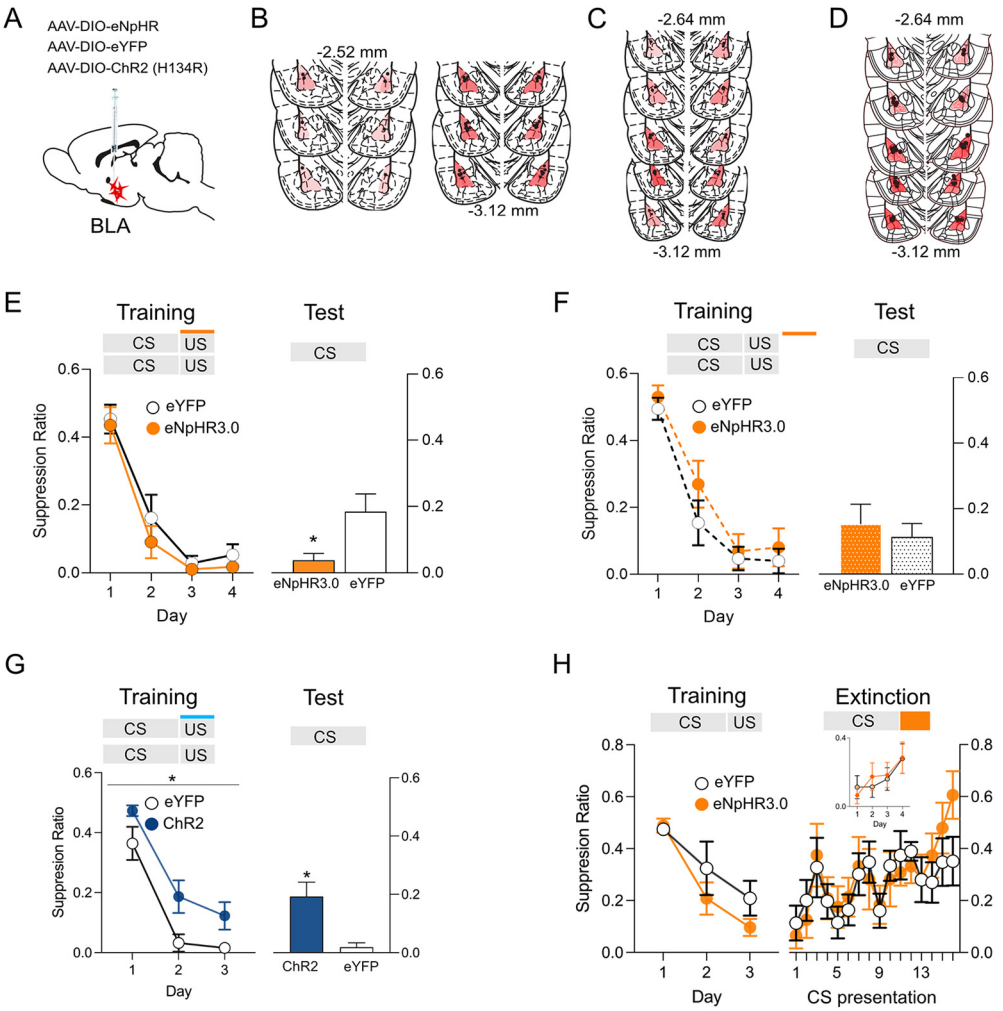

Figure 3. Bidirectional modulation of fear learning by optogenetic manipulation of BLA PV neurons. ***A***, PV-Cre rats received infusions of Cre-dependent eNpHR3.0, eYFP, or ChR2 into BLA and application of fiber optic cannulae into the BLA. ***B–D***, Location of fiber tips in BLA and eNpHR3.0 or ChR2 expression for each rat. Viral spread shown is specific to expression within the BLA and does not show occasional spread into adjacent regions. ***E***, BLA PV photoinhibition during shock US augmented fear learning (eYFP, $n = 8$; eNpHR3.0, $n = 8$). ***F***, BLA PV photoinhibtion during the intertrial interval had no effect (eYFP, $n = 8$; eNpHR3.0, $n = 7$). ***G***, ChR2 ($n = 7$) photoexcitation during the shock US impaired fear learning compared with control (eYFP, $n = 8$). ***H***, BLA PV photoinhibtion during shock omission (eYFP, $n = 7$; eNpHR3.0, $n = 9$) had no effect on fear extinction. Inset, Responding to the first CS of each extinction session. *$p < 0.05$.

groups (no effect of group, $F_{(1,14)} = 0.020$, $p = 0.890$; or group × day interaction, $F_{(1,14)} = 0.065$, $p = 0.802$) despite decreased fear across days (linear trend across day, $F_{(1,14)} = 14.47$, $p < 002$). We also found no differences between groups on any of the four extinction days (largest F value on day 2, $F_{(1,14)} = 0.309$, $p = 0.587$), further confirming that extinction was not influenced by photoinhibition. So, in contrast to the role of BLA PV neurons in fear learning at the time of US delivery, the activity of BLA PV neurons at the time of shock omission is not necessary for fear extinction learning.

Expectation modulation of BLA PV neuron activity

BLA PV activity inhibits principal neurons and constrains fear learning, and this role is observed across different measures of fear in both mice and rats. However, whether activity of PV neurons changes across the course of fear learning and whether it varies with shock expectancy is unknown. Here, we asked whether the US-evoked activity of BLA PV neurons is modulated by expectation. To do this, we used fiber photometry (Gunaydin et al., 2014) to measure Ca^{2+} transients in BLA PV neurons across fear conditioning and then on test during expected (i.e., signaled) versus unexpected (i.e., unsignaled) footshocks.

We expressed Cre-dependent gCaMP7s and fiber optic cannulae in the BLA of PV-Cre rats ($n = 7$; Fig. 4*A*) and subjected them to three days of auditory fear conditioning before a fourth day of fear conditioning, which also served as a test day. We recorded Ca^{2+} transients to the footshock US on the first day of training and on test. Rats acquired fear to the auditory CS across training and test because conditioned suppression decreased across 4 d ($F_{(1,7)} = 83.151$, $p < 0.001$). PV neurons were excited by shock, but this shock-induced PV activity decreased across training (AUC day 1 vs day 4, $t_{(6)} = 2.23$, $p = 0.045$; Fig. 4*B*). At test, rats received the usual CS–US pairings (signaled) and also two additional unsignaled footshock USs. This allowed us to compare, within the same subjects in the same session, BLA PV neuron activity to expected and unexpected footshock USs. The periods when the 95% confidence interval for the population mean ΔF/F did not contain 0% as well as the AUCs for these waveforms are shown in Figure 4, *C* and *D*. There was significantly greater PV activity to the unexpected than expected footshock US (95% confidence interval for signaled vs unsignaled does not include 0%; Fig. 4C, yellow bars; AUC, $t_{(7)} = 3.114$, $p = 0.021$; Fig. 4*D*). This shows the expectation modulation of US-evoked PV BLA interneuron

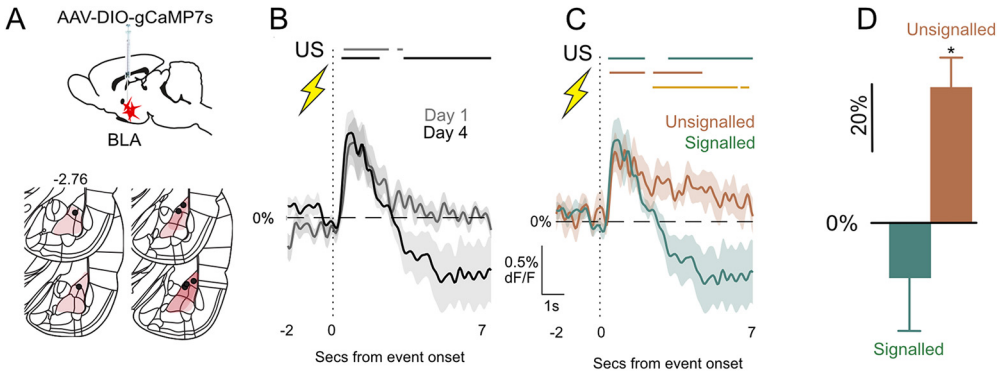

Figure 4. Expectation modulation of BLA PV neurons. ***A***, PV-Cre rats ($n = 7$) received AAV-encoding Cre-dependent gCaMP7s and fiber optic cannulae into the BLA. Viral spread shown is specific to expression within the BLA and does not show occasional spread into adjacent regions. ***B***, Subject-based, signaled US-evoked transients on day 1 and 4 (Test). Bars above transients show periods significantly different to 0% ΔF/F each day ($p < 0.05$). ***C***, Subject-based US-evoked transients on test for unsignaled and signaled footshock. Colored bars above transients show periods significantly different to 0% ΔF/F ($p < 0.05$) for each condition, and yellow bar shows periods of significance between conditions. ***D***, Subject-based AUC ΔF/F 0–7 s after US onset. *$p < 0.05$.

activity during fear learning, with greater responses to unexpected than expected footshocks.

BLA PV neurons are modulated by aversive prediction error

Simple pavlovian fear conditioning designs, like those just used, can provide evidence that BLA PV activity is modulated by expectation. However, they cannot assess whether these variations in BLA PV activity actually relate to variations in the effectiveness of the US as a reinforcer for learning, that is, aversive prediction error. Just because there were greater PV Ca^{2+} transients to the unexpected than expected shock US on test does not mean that different amounts of fear were instructed by the unexpected than expected shock US. This is because measurement of fear in simple fear conditioning using a single CS confounds the accumulated fear to the CS from previous conditioning trials with the change in learning produced by the current trial.

To ask whether BLA PV neurons are modulated by aversive prediction error, we measured Ca^{2+} transients in BLA PV neurons during an associative blocking task, which allows variations in PV neuron activity to be assessed under conditions that yield different amounts of fear learning (Kamin, 1968; McNally and Westbrook, 2006). PV-Cre rats received AAV encoding Cre-dependent gCaMP7s and fiber optic cannulae into the BLA (Fig. 5*A*,*B*). There was exclusive expression of gCaMP7s in PV neurons (Fig. 5*B*) and 28% of PV-IR neurons expressed gCaMP7. The associative blocking procedure uses a two-stage fear conditioning approach to isolate and assess prediction error. During Stage I, rats in the Block group received fear conditioning of a CSA. Rats in the Control group did not receive this training. This Stage I training establishes fear of CSA in group Block. Then, in Stage II, both groups received fear conditioning of a compound CSA and CSB (CSAB). The Block group animals should not learn to fear CSB in Stage II because they have already learned that CSA signals shock, hence the shock US is expected in Stage II (i.e., prediction error is low). In contrast, the Control group animals should learn to fear CSB during Stage II because the shock US is unexpected in Stage II (i.e., prediction error is high).

Precisely this pattern of results was observed (Fig. 5*C*). Group Block ($n = 10$) learned to fear CSA in Stage I ($F_{(1,9)} = 41.00$, $p < 0.001$). Group Block also showed more fear to CSAB than group Control ($n = 9$) in Stage II (main effect of group, $F_{(1,17)} = 41.56$, $p < 0.001$), but group Control did learn to fear CSAB in Stage II (main effect of day, $F_{(1,17)} = 25.56$, $p < 0.001$; group × day interaction, $F_{(1,17)} = 28.32$, $p < 0.001$). Critically, on test, group Control animals were more afraid of CSB than group Block ($F_{(1,17)} = 18.67$, $p < 0.001$). This shows the associative blocking of fear learning; that is, the same aversive footshock US supported different amounts of fear learning, depending on whether it was expected or unexpected.

The average gCaMP7s waveforms to the USs, the periods when the 95% confidence interval for the population mean ΔF/F did not contain 0%, as well as the AUCs for these waveforms, are shown in Figure 5*D–F*. BLA PV neurons showed significant Ca^{2+} transients at US onset during Stage II fear conditioning (Fig. 5*D*). Critically, these transients were greater in group Control when the US was unexpected and fear learning occurred than in group Block when the US was expected and fear learning was blocked. We measured the area under the ΔF/F curve and found that US-evoked Ca^{2+} transients decreased across Stage II (main effect of day, trials, $F_{(1,62)} = 5.197$, $p < 0.026$; subjects, $F_{(1,16)} = 6.835$, $p < 0.019$), and this decrease was greatest in group Control (day × group interaction, trials, $F_{(1,62)} = 4.165$, $p < 0.046$; subjects, $F_{(1,16)} = 6.616$, $p < 0.020$; Fig. 5*D–F*). This shows diminution of US-evoked activity for group Control. Indeed, group Control had significantly greater US-evoked transients than group Block on day 1 (trials, $F_{(1,69)} = 7.74$, $p = 0.007$; subjects, $F_{(1,17)} = 4.75$, $p = 0.04$) but not day 2 (trials, $F_{(1,66)} = 0.32$, $p = 0.75$; subjects, $F_{(1,16)} = 0.21$, $p = 0.65$; Fig. 5*E*, trials; *F*, subjects).

These results show that the differences we observed in US-evoked transients to expected versus unexpected USs in simple fear learning can be extended to a blocking procedure and that prediction error drives variations in US processing by PV neurons during pavlovian fear conditioning. This conclusion may have been strengthened via use of a control that received Stage I training with a third CS paired with shock rather than simple lever-press training. This would better control for any nonassociative effects (e.g., habituation) affecting BLA PV responses to the shock in Stage II of blocking. However, consistent with our previous experiment, PV neurons were strongly excited by an unexpected US (high prediction error) and these responses decreased as the US became expected (low prediction error). Crucially, this experiment shows that this modulation by prediction error is directly related to the effectiveness of the US as a reinforcer.

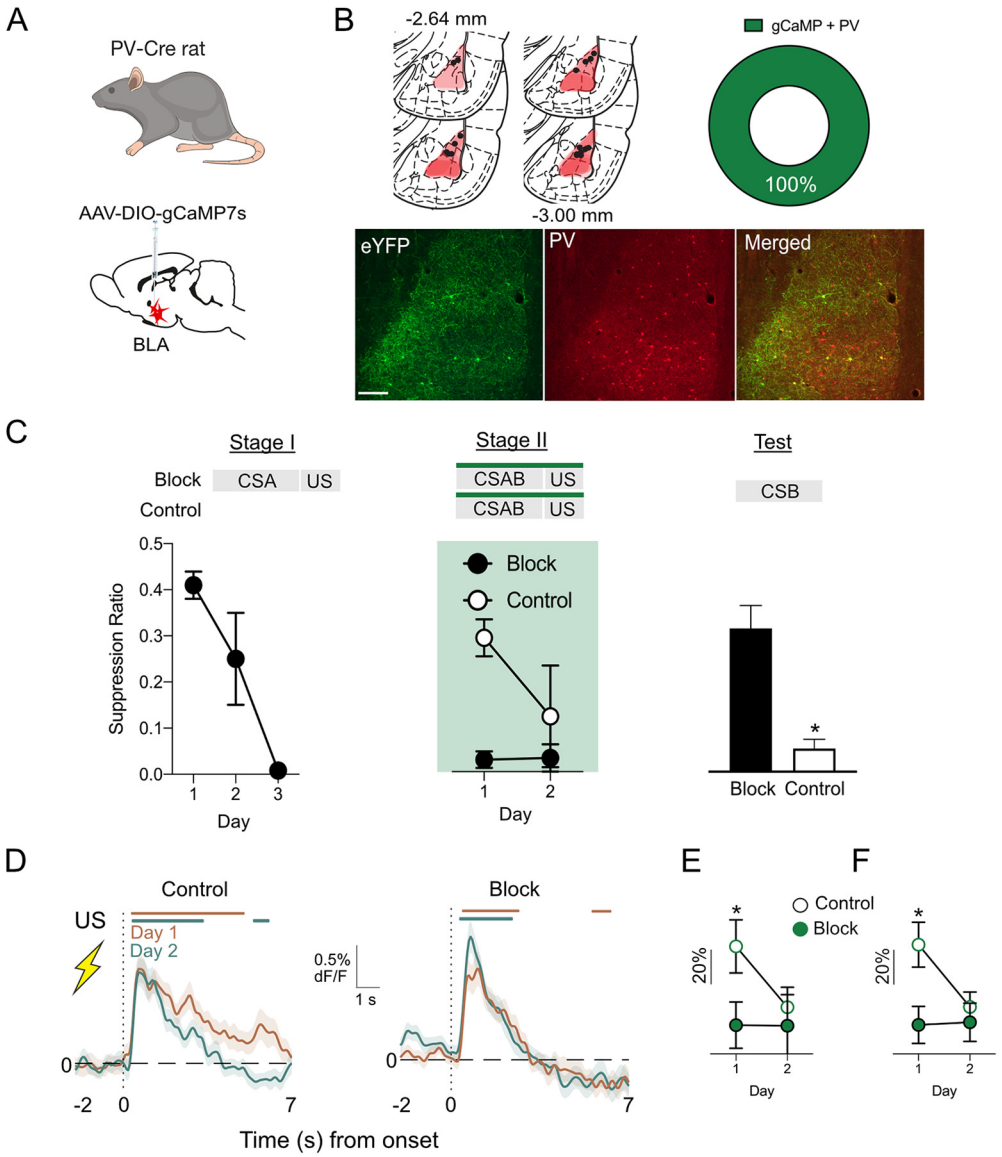

Figure 5. Prediction error modulation of BLA PV neurons. ***A***, ***B***, PV-Cre rats ($n = 19$) received AAV-encoding Cre-dependent gCaMP7s and fiber optic cannulae into the BLA. Location of fiber tips in BLA and gCaMP expression for each rat. Viral spread shown is specific to expression within the BLA and does not show occasional spread into adjacent regions. Two-color immunofluorescence showed gCaMP7s expression in PV neurons ($n = 2$). ***C***, Blocking of associative fear learning. Group Block ($n = 10$) showed more fear to CSAB than group Control ($n = 9$) in Stage II but group Control learned to fear CSAB in Stage II. Group Control were more afraid of CSB on test than group Block. ***D***, Fiber photometry showing US-evoked transients in BLA PV neurons during Stage II of associative blocking for groups Control and Block. Colored bars above transients show periods significantly different to 0% ΔF/F ($p < 0.05$). ***E***, Subject-based ΔF/F 0–7 s after US onset. ***F***, Trial-based ΔF/F 0–7 s after US onset. *$p < 0.05$.

BLA PV neurons constrain fear learning across variations in prediction error

Having demonstrated that aversive prediction error modulates BLA PV neurons, we next asked how BLA PV neurons control fear learning across these variations in prediction error. To do this, we photoinhibited BLA PV neurons at the time of the expected shock US during Stage II of the associative blocking procedure. PV-Cre rats received AAV encoding Cre-dependent eNpHR3.0 ($n = 15$) or eYFP ($n = 15$) and fiber optic cannulae into the BLA (Fig. 6*A*,*B*). They then received the two-stage associative blocking procedure. BLA PV neurons were silenced during US delivery in Stage II. There were four groups: eNpHR3.0-Block, eYFP-Block, eNpHR3.0-Control, and eYFP-Control.

As expected, the Block groups acquired fear to CSA in Stage I (main effect of day, $F_{(1,13)} = 274.60$, $p < 0.001$; Fig. 6*C*). There was no manipulation during Stage I, and the Block-eYFP and Block-eNpHR3.0 groups did not differ during this stage (no main effect of group, $F_{(1,13)} = 0.069$, $p = 0.797$; no group × day interaction, $F_{(1,13)} = 0.034$, $p = 0.857$). During Stage II, the Block groups showed high levels of fear to CSAB, whereas the Control groups learned to fear CSAB (main effect of group, $F_{(1,26)} = 90.41$, $p < 0.05$; main effect of day, $F_{(1,26)} = 49.94$, $p < 0.001$; group × day interaction, $F_{(1,26)} = 43.23$, $p < 0.001$; Fig. 6*C*). There was no effect of photoinhibition of BLA PV neurons during Stage II. At test, the Block groups showed less fear compared with Control groups (main effect group, $F_{(1,26)} = 65.42$, $p < 0.0001$), again demonstrating successful blocking and the role of prediction error in constraining fear association formation. Importantly, silencing BLA PV neurons during the expected shock in Stage II reduced this blocking (group × virus interaction, ($F_{(1,26)} = 8.51$, $p < 0.007$; eNpHR3.0-Block vs eYFP-Block,

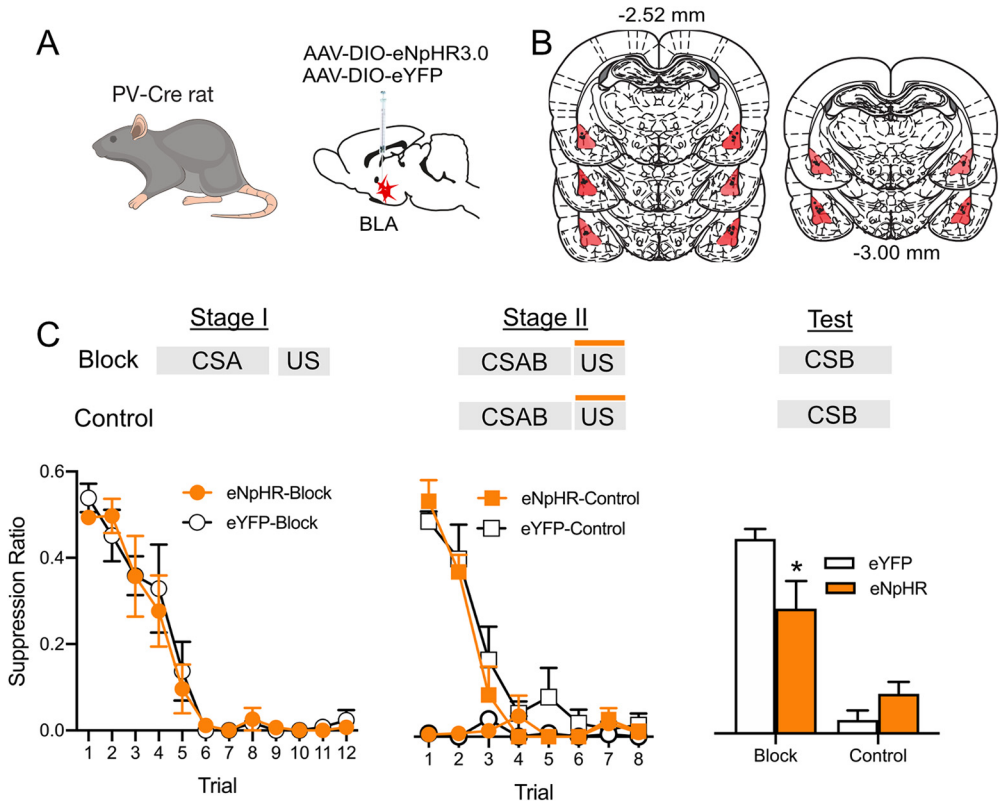

Figure 6. BLA PV neurons constrain association formation under variations in prediction error. ***A***, ***B***, PV-Cre rats received BLA infusions of Cre-dependent eNpHR3.0 or eYFP and fiber optic cannulae into the BLA. Viral spread shown is specific to expression within the BLA and does not show occasional spread into adjacent regions. ***C***, eNpHR3.0-Block ($n = 8$) and eYFP-Block ($n = 7$) both learned fear to CSA in Stage I, and eYFP-Control ($n = 8$) learned to fear CSAB during Stage II. Blocking was demonstrated at test. BLA photoinhibition during the Stage II shock US reduced blocking and restored fear learning to CSB in group eNpHR3.0-Block. *$p < 0.05$.

$F_{(1,13)} = 9.06$, $p = 0.01$; Fig. 6*C*). PV neuron inhibition did not augment learning in the Control group in this experiment (eNpHR3.0-Control vs eYFP-Control, $F_{(1,13)} = 1.25$, $p = 0.285$), in contrast to our earlier experiment. This is unsurprising. The experimental parameters, including the amount of training, US intensity, use of a compound CS, and conditions of testing were optimized to detect associative blocking, not augmentation of *de novo* fear learning.

Discussion

Here, we used the PV-Cre rat (Wright et al., 2021) to study the role of BLA PV neurons in pavlovian fear conditioning and aversive prediction errors. We first confirmed the validity of the PV-Cre rat. Cre-dependent AAVs robustly expressed in BLA neurons with high levels of selectivity to PV neurons, although it is worth noting that less than half of the BLA PV neurons we identified expressed the AAV constructs. This relatively low expression was observed across two different AAVs, so it does not appear to be specific to the choice of AAV, but whether it is unique to the PV-Cre rat or whether it is also observed in the PV-Cre mouse is unknown. We confirmed the electrophysiological properties of these PV neurons as well as the ability of these neurons to inhibit action potential firing in BLA projection neurons. Together, these findings confirm the utility of the PV-Cre rat for studying BLA PV neuron functions.

Amygdala PV neurons have different roles in learning fear and extinction

PV neurons show heterogenous responses to noxious stimuli (Bienvenu et al., 2012). In fear conditioning, single-unit recordings show that some PV neurons can be inhibited by a footshock US to disinhibit BLA projection neurons allowing fear association formation (Wolff et al., 2014). By contrast, in calcium imaging studies, many PV neurons are excited by footshock (Krabbe et al., 2019), and this is consistent with findings that footshock causes rapid inhibitory synaptic input to restrict action potential generation and firing frequency of BLA projection neurons (Windels et al., 2010). Here, we show that at the population level, rat BLA PV neurons are robustly activated by the shock US, *in vitro* excitation of these neurons inhibits BLA projection neurons, and silencing PV neurons during shock USs impairs fear learning whereas exciting PV neurons augments fear learning. Although fiber photometry did not allow us to resolve the activity of individual BLA PV neurons, our findings from photoinhibition and photoexcitation show a key role for shock US-evoked PV neuron activity in constraining fear learning.

In contrast to these effects on fear learning, BLA PV inhibition at the time of shock US omission had no effect on fear extinction learning. Fear extinction learning proceeded normally despite inhibition of BLA PV neurons at the time of the absent but expected US. This was surprising because BLA PV neurons are important for fear extinction. For example, fear extinction remodels mouse BLA PV networks to cause increased perisomatic inhibition onto BLA fear neurons during extinction retrieval (Trouche et al., 2013; Davis et al., 2017). Specifically, PV neurons permit extinction retrieval by balancing two competing local field potential oscillations, one of which (3–6 Hz) is associated with CS-evoked conditioned freezing (Davis et al., 2017). Our findings suggest that despite this role in fear extinction expression, fear extinction learning itself does not depend on

BLA PV activity at the time of US omission. This raises the interesting possibility that the role for BLA PV neurons in fear extinction is linked to changes in CS processing.

The basis for this dissociation in how BLA PV neurons regulate fear and extinction learning is unclear. One possibility is that different populations of PV neurons or different local inhibitory microcircuits are important. PV neurons have diverse firing properties and form multiple networks in the BLA, including PV neuron → projection neuron, projection neuron → PV neuron, and PV neuron → other interneuron networks (Woodruff and Sah, 2007b). There are also differences in fear-conditioning-related plasticity between PV neurons located across the amygdala (Lucas et al., 2016). This considerable diversity in how PV neurons contribute to the intrinsic circuitry of the BLA, and in PV neuron plasticity, could underpin these different roles in learning about aversive shock USs and absence of these shocks (Morrison et al., 2016).

Variations in US-evoked activity in PV neurons

BLA PV neurons were strongly excited by an unexpected US, and these responses decreased as the US became expected. This change in sensitivity to the US was not because of US habituation because PV activity could be rescued by presentations of an unsignaled US. Instead, this expectation-modulation of PV activity was directly related to variations in fear prediction error, with stronger excitation to a US that supported fear learning (high prediction error) than to the same US that did not (low prediction error). It is also worth noting that these changes were observed by averaging PV activity across seconds following event onset. Coupled with the slow kinetic profile of gCaMP7s (Dana et al., 2019), our measure prioritized signal sensitivity over temporal specificity.

Although clearly demonstrating modulation by prediction error, our findings argue against the possibility that BLA PV neurons compute this error. If PV neurons computed a prediction-error signal to gate US activity of BLA projection neurons, then PV neurons should show the greatest excitation at the time of the expected shock US when projection neurons require the greatest inhibition. Indeed, GABA neurons that regulate reward prediction error signaling in VTA dopamine neurons show precisely this activity profile. During appetitive conditioning, VTA dopamine neurons are recruited by surprising or unexpected rewards but not by expected rewards (Schultz et al., 1997; Schultz, 2006). VTA GABA neurons show a profile of ramping activity at CS onset, peaking at the moments of US delivery to inhibit both US-evoked responses in VTA dopamine neurons and reward learning (Cohen et al., 2012; Eshel et al., 2015). We did not observe this. Instead, we found the opposite. US-evoked activity in PV neurons was greatest for an unexpected shock US and decreased as prediction error decreased. This same profile of prediction-error-related changes has been reported in rat single-unit recordings of slow (putative projection) and fast (putative interneurons) firing BLA neurons (Johansen et al., 2010), in mouse single-unit recordings of identified VIP interneurons (Krabbe et al., 2019), and in mouse BLA (McHugh et al., 2014) as well as human amygdala fMRI BOLD signals (Eippert et al., 2012; Michely et al., 2020). It appears to be a common feature of distinct BLA cell types despite these cell types having distinct roles in fear learning (Letzkus et al., 2015; Tovote et al., 2015; Krabbe et al., 2019).

One interesting feature of these results was that BLA PV neuron function in fear learning was preserved across these changes in US sensitivity. If PV inhibition scales with incoming excitatory input, strong PV inhibition in response to strong excitatory input from an unexpected shock could serve to limit fear learning. On the other hand, weak PV inhibition in response to weak excitatory input from an expected shock may permit the updating of fear associations in the face of any new additional information such as changes to features of the US (Betts et al., 1996). Fear learning depends on the aversive valence of the footshock US, but it also depends on the specific sensory features of the US such as duration and precise location, which are critical for ensuring that defensive behavior is appropriately directed to protect the organism (Brandon et al., 1994). The BLA is essential to learning about these specific sensory features (Balleine and Killcross, 2006). Variations in these sensory features (i.e., identity prediction errors) allow learning about changes in US identity, which is dissociable from learning about the aversive value of US identity (Betts et al., 1996; Bradfield and McNally, 2008). Thus, PV neurons could act to maintain selectivity of BLA learning circuits to the precise sensory features of the US despite variations in the overall strength of US inputs during conditioning (Ferguson and Cardin, 2020), thereby allowing updating of fear associations when these features change. However, this awaits further investigation.

Conclusions

Here, we used the PV-Cre rat (Wright et al., 2021) to study the role of BLA PV neurons in pavlovian fear conditioning and aversive prediction errors. We show that BLA PV neurons control learning about aversive events but not learning about omission of these events. Furthermore, we show changes in sensitivity of BLA PV neurons to the US across conditioning so that US-evoked activity of BLA PV neurons is modulated by US expectation and specifically by aversive prediction error. We suggest that this enables BLA fear-learning circuits to retain selectivity for specific US sensory features across variations in US expectation, permitting the rapid updating of fear associations when these features change.

References

Annau Z, Kamin LJ (1961) The conditioned emotional response as a function of the intensity of the US. J Comp Physiol Psychol 54:428–432.

Balleine BW, Killcross S (2006) Parallel incentive processing: an integrated view of amygdala function. Trends Neurosci 29:272–279.

Betts SL, Brandon SE, Wagner AR (1996) Dissociation of the blocking of conditioned eyeblink and conditioned fear following a shift in US locus. Anim Learn Behav 24:459–470.

Bevins RA, Ayres JJB (1991) Two issues in pavlovian fear conditioning: selective fear of bright vs. dark, and CS determinants of CR form. Behav Processes 24:211–218.

Bienvenu TC, Busti D, Magill PJ, Ferraguti F, Capogna M (2012) Cell-type-specific recruitment of amygdala interneurons to hippocampal theta rhythm and noxious stimuli in vivo. Neuron 74:1059–1074.

Bradfield L, McNally GP (2008) Unblocking in pavlovian fear conditioning. J Exp Psychol Anim Behav Process 34256–265.

Brandon SE, Betts SL, Wagner AR (1994) Discriminated lateralized eyeblink conditioning in the rabbit: an experimental context for separating specific and general associative influences. J Exp Psychol Anim Behav Process 20:292–307.

Cohen JY, Haesler S, Vong L, Lowell BB, Uchida N (2012) Neuron-type-specific signals for reward and punishment in the ventral tegmental area. Nature 482:85–88.

Dana H, Sun Y, Mohar B, Hulse BK, Kerlin AM, Hasseman JP, Tsegaye G, Tsang A, Wong A, Patel R, Macklin JJ, Chen Y, Konnerth A, Jayaraman V, Looger LL, Schreiter ER, Svoboda K, Kim DS (2019) High-performance calcium sensors for imaging activity in neuronal populations and microcompartments. Nat Methods 16:649–657.

Davis P, Zaki Y, Maguire J, Reijmers LG (2017) Cellular and oscillatory substrates of fear extinction learning. Nat Neurosci 20:1624–1633.
Eippert F, Gamer M, Büchel C (2012) Neurobiological mechanisms underlying the blocking effect in aversive learning. J Neurosci 32:13164–13176.
Eshel N, Bukwich M, Rao V, Hemmelder V, Tian J, Uchida N (2015) Arithmetic and local circuitry underlying dopamine prediction errors. Nature 525:243–246.
Fanselow MS (1998) Pavlovian conditioning, negative feedback, and blocking: mechanisms that regulate association formation. Neuron 20:625–627.
Fanselow MS, Poulos AM (2005) The neuroscience of mammalian associative learning. Annu Rev Psychol 56:207–234.
Ferguson KA, Cardin JA (2020) Mechanisms underlying gain modulation in the cortex. Nat Neurosci 21:80–92.
Gunaydin LA, Grosenick L, Finkelstein JC, Kauvar IV, Fenno LE, Adhikari A, Lammel S, Mirzabekov JJ, Airan RD, Zalocusky KA, Tye KM, Anikeeva P, Malenka RC, Deisseroth K (2014) Natural neural projection dynamics underlying social behavior. Cell 157:1535–1551.
Herry C, Johansen JP (2014) Encoding of fear learning and memory in distributed neuronal circuits. Nat Neurosci 17:1644–1654.
Jean-Richard-dit-Bressel P, Clifford CWG, McNally GP (2020) Analyzing event-related transients: confidence intervals, permutation tests, and consecutive thresholds. Front Mol Neurosci 13:14.
Johansen JP, Tarpley JW, Ledoux JE, Blair HT (2010) Neural substrates for expectation-modulated fear learning in the amygdala and periaqueductal gray. Nat Neurosci 13:979–986.
Kamin LJ (1968) "Attention-like" processes in classical conditioning. In: Miami Symposium on the prediction of behavior: Aversive stimulation. (Jones MR, ed), pp 9–33. Coral Gables, FL: University of Miami Press.
Krabbe S, Gründemann J, Lüthi A (2018) Amygdala inhibitory circuits regulate associative fear conditioning. Biol Psychiatry 83:800–809.
Krabbe S, Paradiso E, d'Aquin S, Bitterman Y, Courtin J, Xu C, Yonehara K, Markovic M, Müller C, Eichlisberger T, Gründemann J, Ferraguti F, Lüthi A (2019) Adaptive disinhibitory gating by VIP interneurons permits associative learning. Nat Neurosci 22:1834–1843.
Letzkus JJ, Wolff SBE, Lüthi A (2015) Disinhibition, a circuit mechanism for associative learning and memory. Neuron 88:264–276.
Li SSY, McNally GP (2014) The conditions that promote fear learning: prediction error and pavlovian fear conditioning. Neurobiol Learn Mem 108:14–21.
Lucas EK, Jegarl AM, Morishita H, Clem RL (2016) Multimodal and site-specific plasticity of amygdala parvalbumin interneurons after fear learning. Neuron 91:629–643.
Maren S, Quirk GJ (2004) Neuronal signalling of fear memory. Nat Rev Neurosci 5:844–852.
McDonald AJ (1992) Cell types and intrinsic connections of the amygdala. In: The amygdala: neurobiological aspects of emotion, memory, and mental dysfunction (AggletonJ P, ed), pp 67–96. New York: Wiley.
McDonald AJ, Betette RL (2001) Parvalbumin containing neurons in the rat basolateral amygdala: morphology and co-localization of calbindin-D (28k). Neuroscience 102:413–425.
McHugh SB, Barkus C, Huber A, Capitão L, Lima J, Lowry JP, Bannerman DM (2014) Aversive prediction error signals in the amygdala. J Neurosci 34:9024–9033.
McNally GP, Johansen JP, Blair HT (2011) Placing prediction into the fear circuit. Trends Neurosci 34:283–292.
McNally GP, Westbrook RF (2006) Predicting danger: the nature, consequences, and neural mechanisms of predictive fear learning. Learn Mem 13:245–253.
Michely J, Rigoli F, Rutledge RB, Hauser TU, Dolan RJ (2020) Distinct processing of aversive experience in amygdala subregions. Biol Psychiatry Cogn Neurosci Neuroimaging 5:291–300.
Morrison DJ, Rashid AJ, Yiu AP, Yan C, Frankland PW, Josselyn SA (2016) Parvalbumin interneurons constrain the size of the lateral amygdala engram. Neurobiol Learn Mem 135:91–99.
Namburi P, Beyeler A, Yorozu S, Calhoon GG, Halbert SA, Wichmann R, Holden SS, Mertens KL, Anahtar M, Felix-Ortiz AC, Wickersham IR, Gray JM, Tye KM (2015) A circuit mechanism for differentiating positive and negative associations. Nature 520:675–678.
Ozawa M, Davis P, Ni J, Maguire J, Papouin T, Reijmers L (2020) Experience-dependent resonance in amygdalo-cortical circuits supports fear memory retrieval following extinction. Nat Commun 11:4358.
Ozawa T, Johansen JP (2018) Learning rules for aversive associative memory formation. Curr Opin Neurobiol 49:148–157.
Ozawa T, Ycu EA, Kumar A, Yeh LF, Ahmed T, Koivumaa J, Johansen JP (2017) A feedback neural circuit for calibrating aversive memory strength. Nat Neurosci 20:90–97.
Paxinos G, Watson C (2007) The rat brain in stereotaxic coordinates. Amsterdam: Elsevier.
Polepalli JS, Gooch H, Sah P (2020) Diversity of interneurons in the lateral and basal amygdala. npj Sci Learn 5:10.
Polepalli JS, Sullivan RKP, Yanagawa Y, Sah P (2010) A specific class of interneuron mediates inhibitory plasticity in the lateral amygdala. J Neurosci 30:14619–14629.
Rainnie DG, Mania I, Mascagni F, McDonald AJ (2006) Physiological and morphological characterization of parvalbumin-containing interneurons of the rat basolateral amygdala. J Comp Neurol 498:142–161.
Sah P, Faber ESL, Lopez De Armentia M, Power J (2003) The amygdaloid complex: anatomy and physiology. Physiol Rev 83:803–834.
Schultz W (2006) Behavioral theories and the neurophysiology of reward. Annu Rev Psychol 57:87–115.
Schultz W, Dayan P, Montague PR (1997) A neural substrate of prediction and reward. Science 275:1593–1598.
Sengupta A, Winters B, Bagley EE, McNally GP (2016) Disrupted prediction error links excessive amygdala activation to excessive fear. J Neurosci 36:385–395.
Sengupta A, Yau JOY, Jean-Richard-Dit-Bressel P, Liu Y, Millan EZ, Power JM, McNally GP (2018) Basolateral amygdala neurons maintain aversive emotional salience. J Neurosci 38:3001–3012.
Tovote P, Fadok JP, Lüthi A (2015) Neuronal circuits for fear and anxiety. Nat Rev Neurosci 16:317–331.
Trouche S, Sasaki JM, Tu T, Reijmers LG (2013) Fear extinction causes target-specific remodeling of perisomatic inhibitory synapses. Neuron 80:1054–1065.
Windels F, Crane JW, Sah P (2010) Inhibition dominates the early phase of up-states in the basolateral amygdala. J Neurophysiol 104:3433–3438.
Wolff SBE, Gründemann J, Tovote P, Krabbe S, Jacobson GA, Müller C, Herry C, Ehrlich I, Friedrich RW, Letzkus JJ, Lüthi A (2014) Amygdala interneuron subtypes control fear learning through disinhibition. Nature 509:453–458.
Woodruff AR, Sah P (2007a) Inhibition and synchronization of basal amygdala principal neuron spiking by parvalbumin-positive interneurons. J Neurophysiol 98:2956–2961.
Woodruff AR, Sah P (2007b) Networks of parvalbumin-positive interneurons in the basolateral amygdala. J Neurosci 27:553–563.
Wright AM, Zapata A, Hoffman AF, Necarsulmer JC, Coke LM, Svarcbahs R, Richie CT, Pickel J, Hope BT, Harvey BK, et al. (2021) Effects of withdrawal from cocaine self-administration on rat orbitofrontal cortex parvalbumin neurons expressing cre recombinase: sex-dependent changes in neuronal function and unaltered serotonin signaling. eNeuro 8: ENEURO.0017–21.
Wright KM, Jhou TC, Pimpinelli D, McDannald MA (2019) Cue-inhibited ventrolateral periaqueductal gray neurons signal fear output and threat probability in male rats. Elife 8:e50054.
Yau JO-Y, McNally GP (2015) Pharmacogenetic excitation of dorsomedial prefrontal cortex restores fear prediction error. J Neurosci 35:74–83.
Yau JO-Y, McNally GP (2018a) Rules for aversive learning and decision-making. Current Opin Behav Sci 26:1–8.
Yau JOY, McNally GP (2018b) Brain mechanisms controlling pavlovian fear conditioning. J Exp Psychol Anim Learn Cogn 44:341–357.